Electronic Supplementary Information (ESI)

Efficient luminescent copper(I) iodide complexes with crystallization-induced emission enhancement (CIEE) caused by π-π interaction

Mingxue Yang,[a,c] Xu-Lin Chen*[b] and Can-Zhong Lu*[a,b]

a. State Key Laboratory of Structural Chemistry, Fujian Institute of Research on the Structure of Matter, Chinese Academy of Sciences, Fuzhou, Fujian, 350002, China.
b. Xiamen Institute of Rare-earth Materials, Haixi Institute, Chinese Academy of Sciences, Xiamen, Fujian, 361021, China.
c. University of Chinese Academy of Sciences, Beijing,100049, China.
E-mail: czlu@fjirsm.ac.cn; xlchem@fjirsm.ac.cn

Contents

Synthesis & Characteristics

All the starting chemicals are purchased from reagent manufacturers and are chemical pure without further purification unless specified.

a) Characteristic Instruments and methods

- Nuclear Magnetic Resonance (NMR)

^{1}H NMR was performed by Bruker Avance III 400MHz NMR Spectroscopy.

- Crystallography

Crystallography data were obtained from Rigaku SuperNova, with CCD detector and X-ray source of Cu K_α (λ=1.54184Å). Crystal resolution were carried out by Olex2 program (ver.1.2.10) equipping ShelXL-2016 package.[1-3]

- Powder X-ray diffraction (PXRD)

PXRD was performed on Rigaku MiniFlex-600. The sample holder was a silicon wafer with a small indentation in the center.

- Thermodynamics Analysis

Thermogravimetry - Differential Scanning Calorimeter (TG-DSC) diagram was performed by Mettler-Toledo TGA/DSC 1 STARe. The experiment was taken under nitrogen atmosphere. Alumina crucibles were used and the heating rate was 10°C / min.

- Photoluminescence properties

Photoluminescent properties were measured by Horiba Jobin-Yvon FluoroMax-4 fluorescence spectrometer.
The lifetime of each sample was characterized by Edinburgh Instruments FLS980 UV/V/NIR Fluorescence Spectrometer. 375 nm laser was served as the light source.

- Calculation

Density Function Theory (DFT) and Time-dependent DFT (TD-DFT), with B3LYP/6-31(d) level, was adopted and calculations were performed by Gaussian 09 program (version D.01)[4]. Composition analysis and Natural Transition Orbitals (NTO) analysis were carried out by MultiWfn[5]. Frontier orbitals were depicted by VMD[6]. Crystal structure data were utilized without further optimization.

b) Synthesis

1. N Ligand (2-methyl-6-(1H-pyrazol-1-yl)pyridine) was synthesized by a previously reported method.[7]

2. Complex **1** was synthesized as follows:
In a 20 mL serum bottle add 10 mL of dichloromethane, 0.035 g (0.22 mmol) of N ligand, after stirring for 5 minutes, 0.019 g of CuI (0.10 mmol) was added into the solution. CuI gradually disappeared, followed by the precipitation of yellow solid. After 10 minutes' agitating, the mixture was filtered and washed by acetonitrile and hexane. The yellow powder was collected after dryness. Product was 0.028 g. (yield: 80.1%) ^{1}H NMR (400 MHz, DMSO-d_6) δ 8.92 (s, 1H), 8.05 (t, J = 7.8 Hz, 2H), 7.97 (s, 1H), 7.41 (s, 1H), 6.80 (s, 1H), 2.62 (s, 3H). Element Analysis: C 30.86; H 2.61; N 11.98 (Calc: C, 30.92; H, 2.59; N, 12.02)

The **contact method** for cultivating crystalline complex **1** is as follows:
Into a 20 mL of serum bottle the DCM solution of N ligand, buffer layer that consists of DCM and CH_3CN in volumetric ratio of 1:1, and acetonitrile solution of CuI were carefully flowed down the wall, respectively. The volume of each part was 5 mL and the amount of the two solute counterparts were equal. Make sure the boundary of each layer be observed.

3. Complex **2** was synthesized as follows:
In a 20 mL serum bottle add 10 mL of dichloromethane, 0.032 g (0.20 mmol) of N ligand and 0.027 g (0.10 mmol) of PPh_3, after stirring for 5 minutes, 0.019 g of CuI (0.10 mmol) was added into the solution. CuI gradually disappeared, and transparent yellow solution was formed. After 10 minutes' agitating, the mixture was filtered, evaporated under reduced pressure and washed by hexane. The pale yellow powder was collected after dryness. Product was 0.030 g. (yield: 49.0%) ^{1}H NMR (400 MHz, Chloroform-*d*) δ 8.53 (s, 1H), 7.78 (t, *J* = 7.9 Hz, 1H), 7.70 (d, *J* = 1.6 Hz, 1H), 7.64 (d, *J* = 8.2 Hz, 1H), 7.50 (t, *J* = 8.8 Hz, 6H), 7.36 (t, *J* = 7.3 Hz, 3H), 7.28 (t, *J* = 7.3 Hz, 6H), 7.10 (d, *J* = 7.5 Hz, 1H), 6.50 (dd, *J* = 2.7, 1.7 Hz, 1H), 2.70 (s, 3H). Element Analysis: C 53.08; H 3.98; N 7.01. (Calc: C, 53.00; H, 3.95; N, 6.87)

4. Complex **3** was synthesized as follows:
In a 20 mL serum bottle add 10 mL of acetonitrile, 0.019 g of CuI (0.10 mmol) was added into the liquid. The mixture was treated by ultra-sonication for 5 minutes so as to completely dissolve CuI. After that, 0.027 g (0.10 mmol) of PPh_3 was added into the solution. Stir for 5 minutes and then stop. A few

moments later, the single crystal complex **3** precipitated. ^{1}H NMR (400 MHz, DMSO-d_6) δ 7.44 (dt, J = 12.4, 3.8 Hz). Product was 0.040 g. (yield: 88.3%) Element Analysis: C 47.80; H 3.41.(Calc: C, 47.75; H, 3.34)

Synthetic Strategy

Table S1 Selected conditions and results of the control test

Sequence	Solvent	Volume	CuI:N^N[a]:PPh$_3$	Crystal[b]
N^N→PPh$_3$	DCM[c]	10 mL	1:1:1	**3**
PPh$_3$→N^N	DCM	10 mL	1:1:1	**3**
N^N→PPh$_3$	CH$_3$CN	10 mL	1:1:1	**3**
N^N→PPh$_3$	DCM	5 mL	1:1:1	**3**
		15 mL		**3**
		20 mL		**3**
N^N→PPh$_3$	DCM	10 mL	1:4:1	**1**
			1:3:1	**2**
			1:2:1	**2**
			1:1:2	**3**
			1:1:3	**3**
			1:1:4	**3**

a. N^N refers to N ligand. b. Crystals that firstly and mainly come out. c. Dichloromethane.

Powder X-ray Diffraction

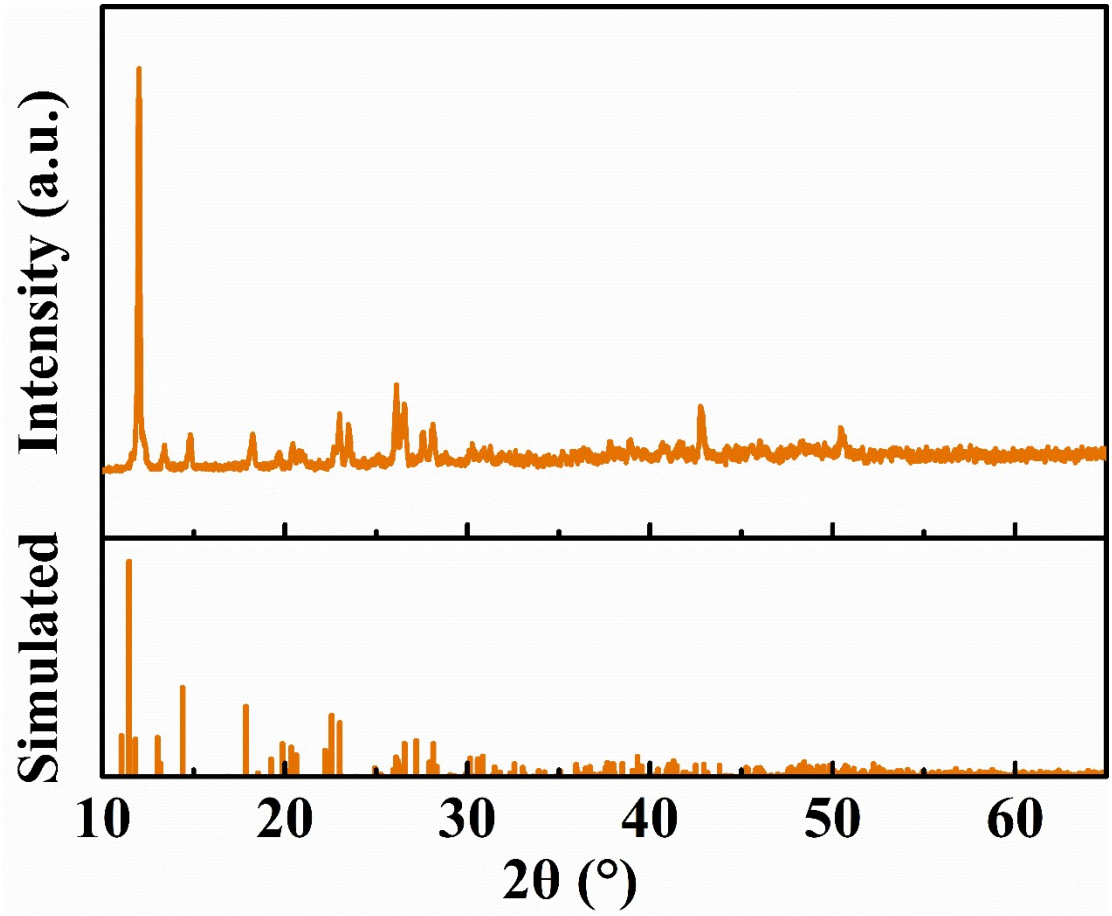

Fig. S1 Powder X-ray diffraction of complex **1**. A simulated pattern was shown under the pattern of the crystallized sample.

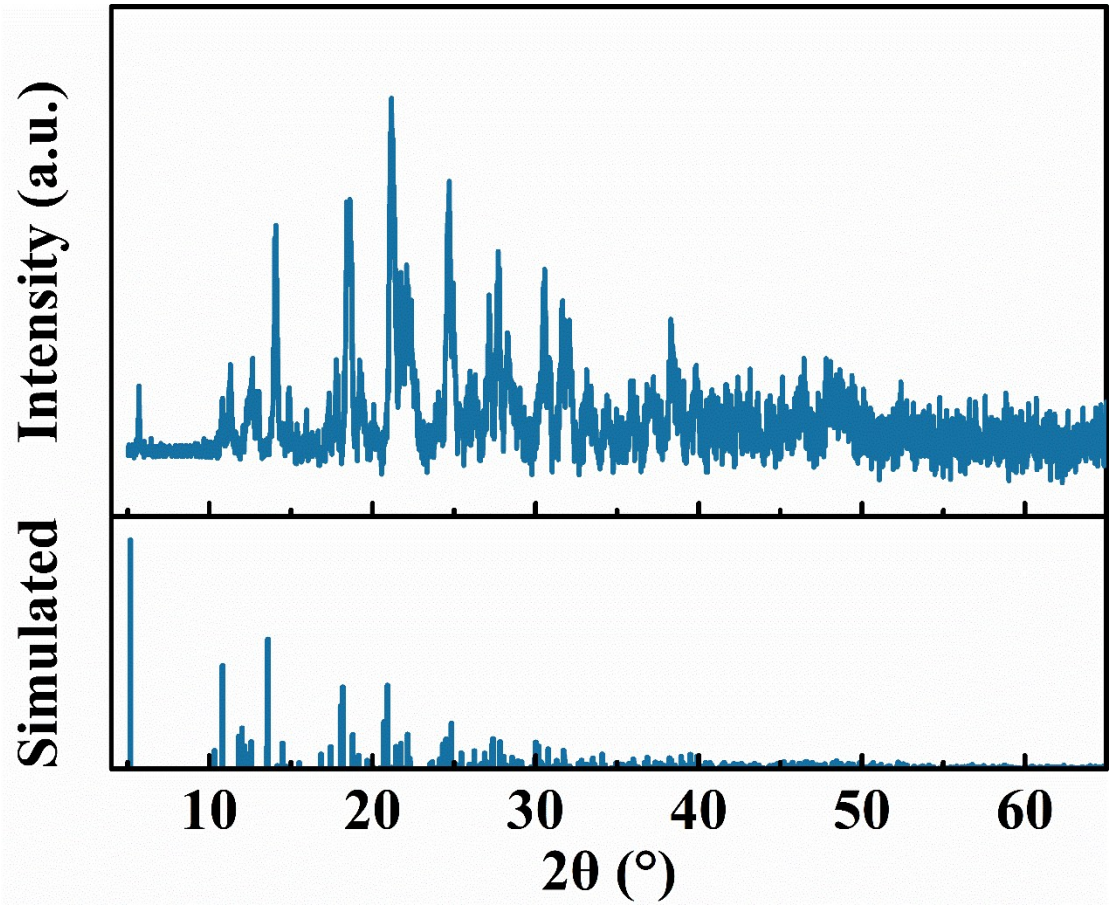

Fig. S2 Powder X-ray diffraction of complex **2**. A simulated pattern was shown under the pattern of the crystallized sample.

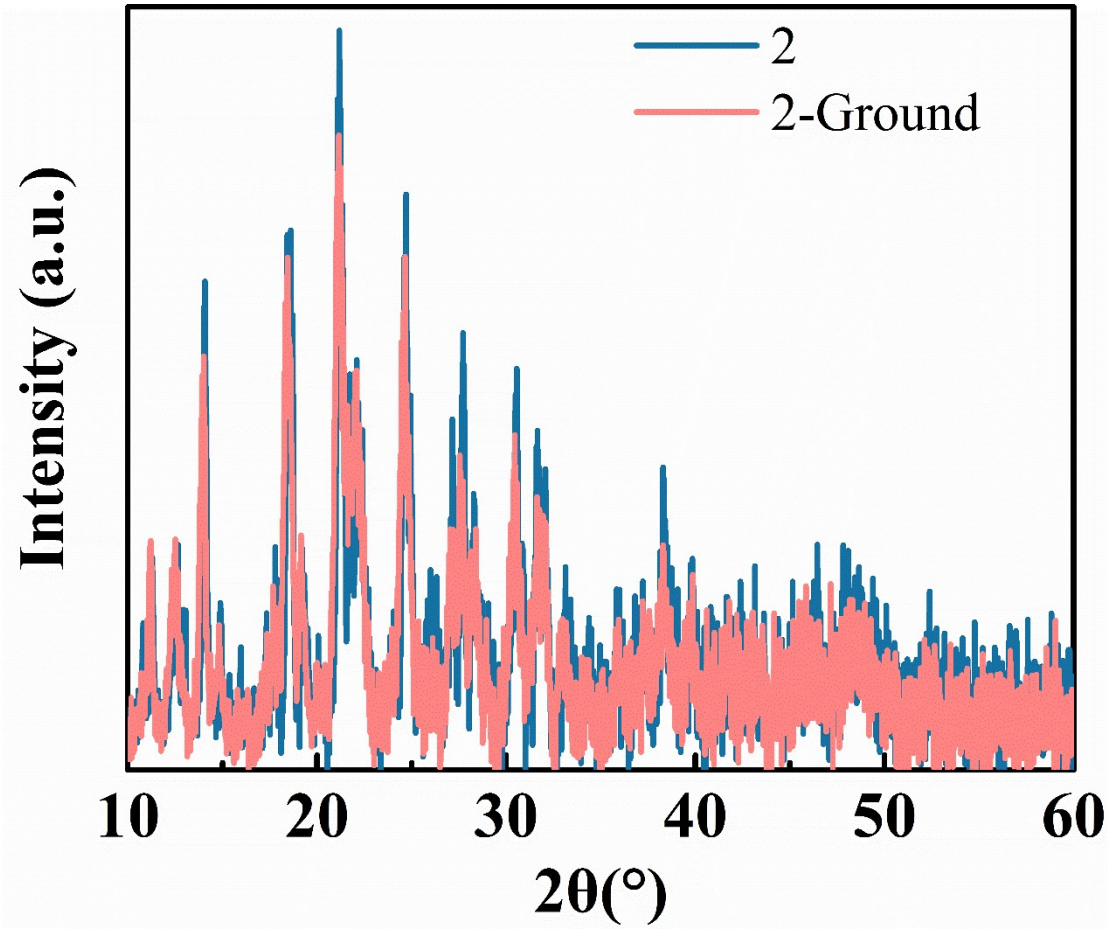

Fig. S3 A comparison between as-synthesized and ground complex **2**.

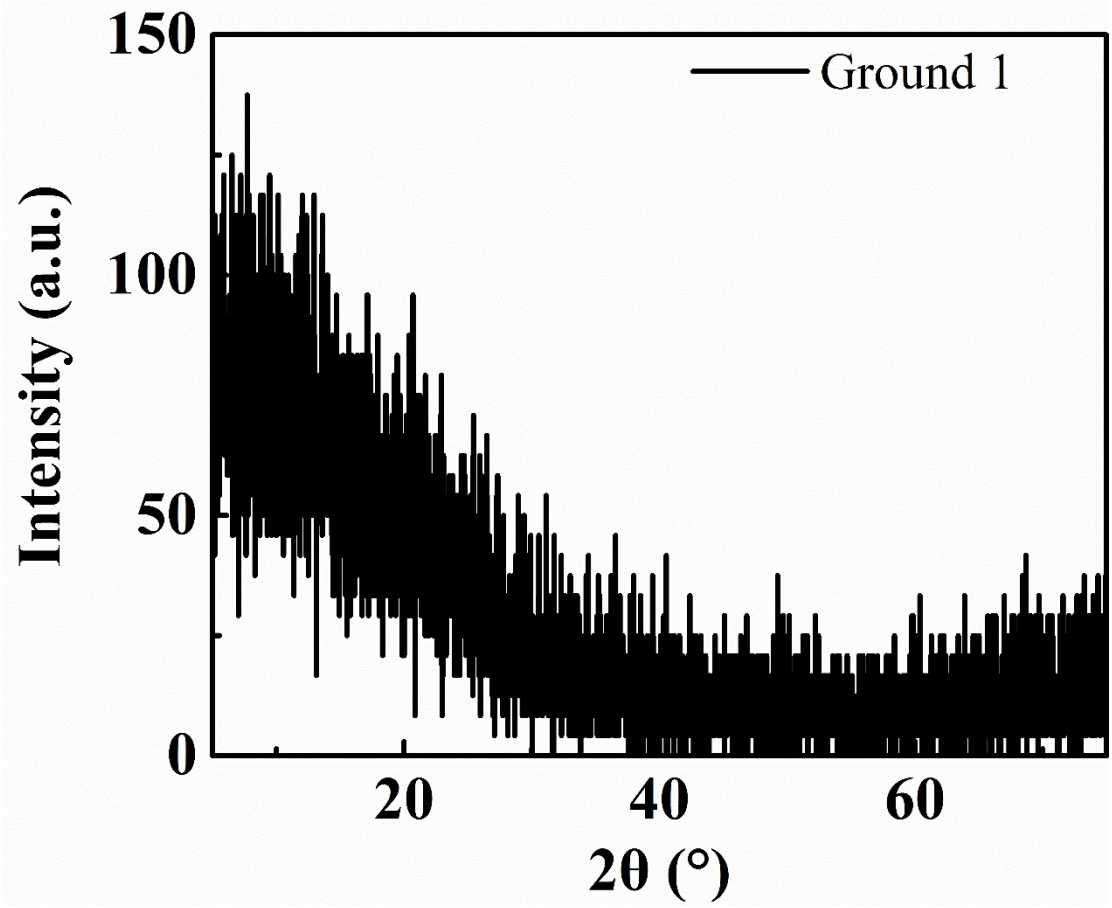

Fig. S4 Powder X-ray diffraction pattern of ground complex **1**.

Method of recovering complex 1:

Since the insolubility for most of the solvents of complex **1**, recovery of complex **1** was performed by stirring the ground powder in DCM for 10 minutes. The suspension gradually turned brighter under the UV-light. The mixture was then filtered, dried at 50 °C in an oven and cooled down to room temperature before the tests in the following cycles.

Thermodynamics Analysis

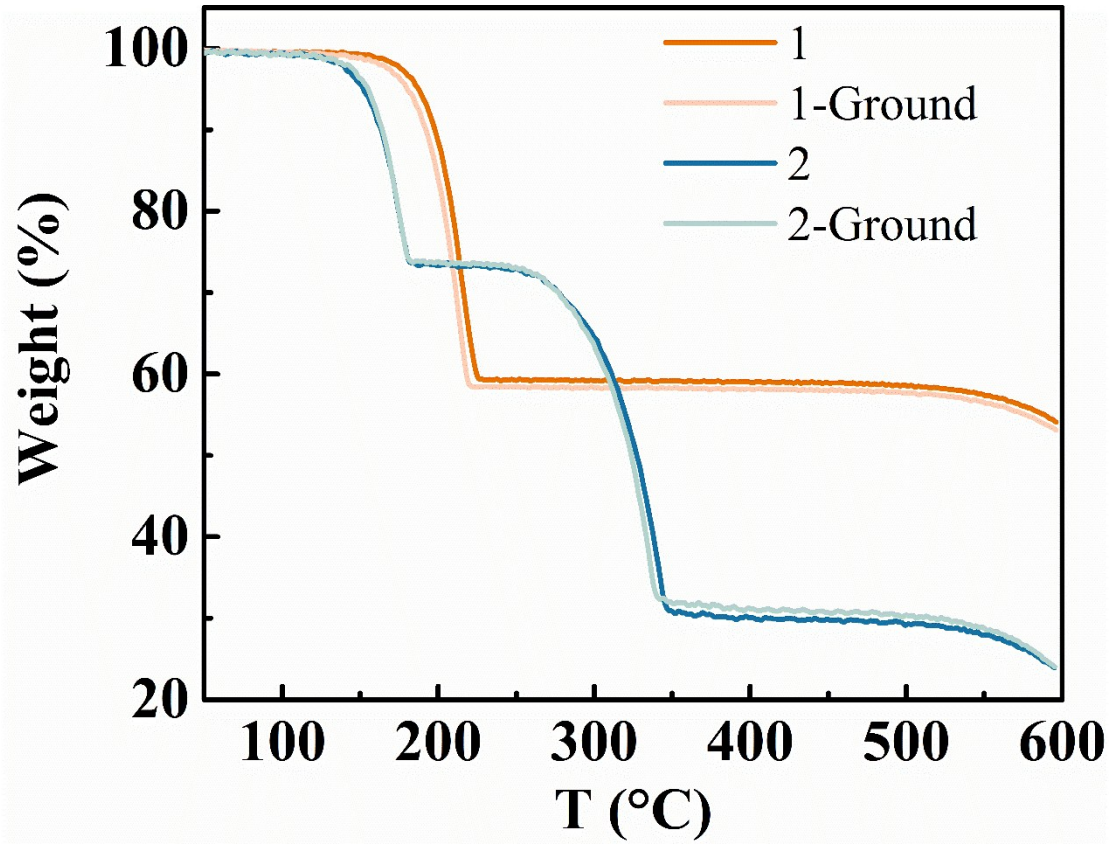

Fig. S5 Thermogravimetric analysis (TGA) curves for complex **1** and **2**, and their corresponding ground samples. Little changes existed between each sample and respective ground one. For complex **1** and **1**-ground, the weight loss at around 230 K should be attributed to the decomposition of N ligand, which is also the process occurred in the first staircase of complex **2** and **2**-ground. The second weight loss for complex **2** and **2**-ground is the loss of PPh_3 ligand.

Scanning Electron Microscope (SEM) pattern

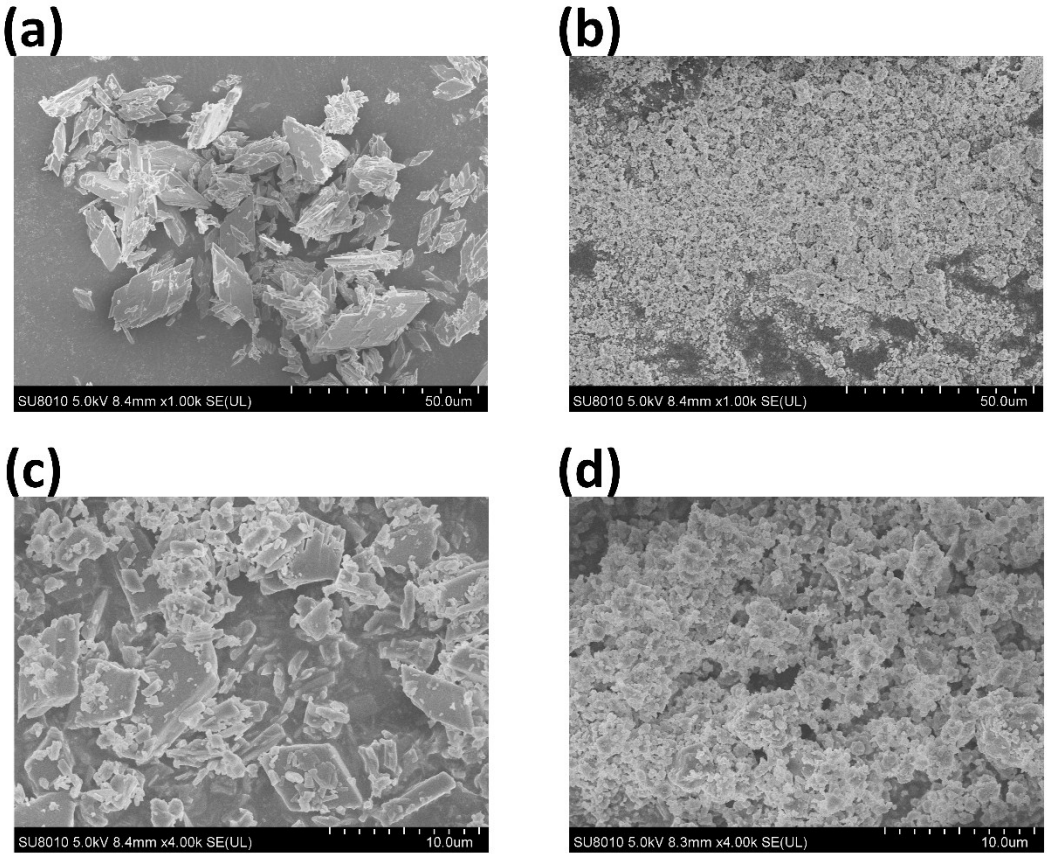

Fig S6 SEM patterns of (a) crystalline **1**, (b) ground **1**, (c) crystalline **2** and (d) ground **2**. It is obvious that (a) and (c) were in good shapes, (b) was totally amorphous and (d) was the mixture of crystalline and amorphous sample.

X-ray photoelectron spectroscopy (XPS)

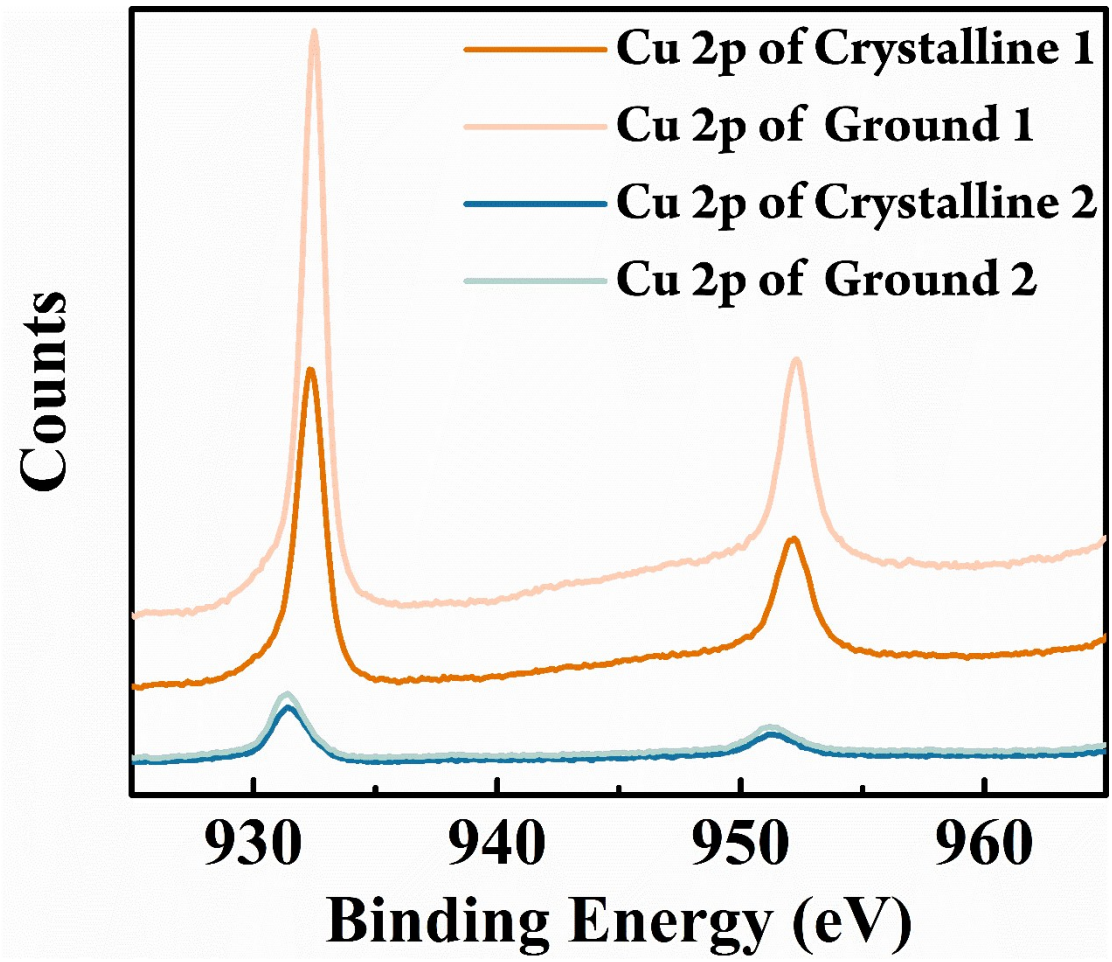

Fig. S7 XPS spectra for Cu 2p orbital of crystalline and ground **1** and **2.** According to the data (https://xpssimplified.com/elements/copper.php), no strong Cu^{2+} satellite peaks were found in all the spectra, indicating that Cu(I) in each sample remained unchanged before and after grinding.

Theoretical Calculation

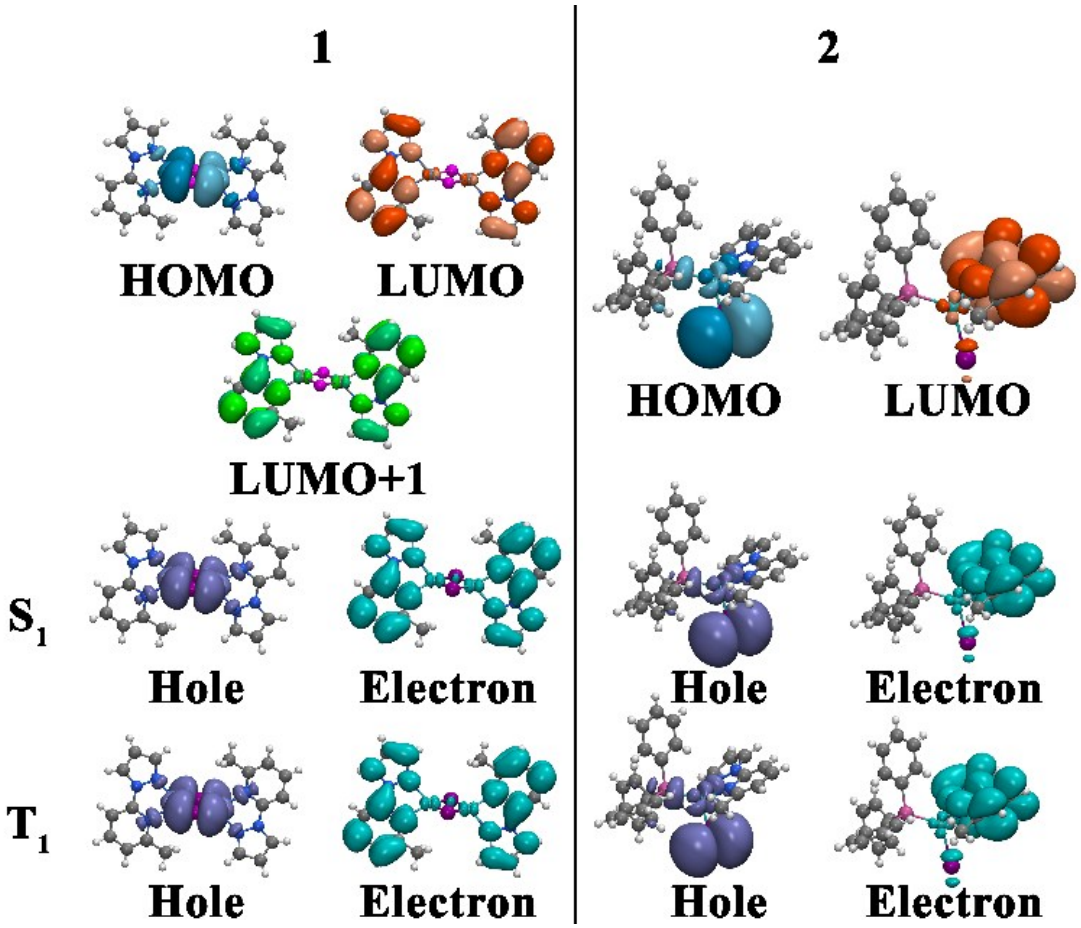

Fig. S7 Molecular orbitals of complex **1** and **2**. Highest occupied molecular orbitals (HOMO), lowest unoccupied molecular orbitals (LUMO), and the molecular orbital related to the lowest excited state transitions was drawn. Hole and electron distributions of complex **1** and **2** were also depicted using natural transition orbitals (NTO).

Table S2 Component analysis of orbitals participating in the lowest excited transitions (S_1 and T_1).

Component	1		2	
	HOMO	LUMO+1	HOMO	LUMO
Cu	58.02%	3.29%	15.07%	3.65%
I	34.56%	2.59%	73.60%	1.50%
N ligand	7.42%	94.12%	2.94%	92.23%
PPh_3			8.39%	2.61%

Table S3 Component analysis of natural transition orbitals (NTOs) and characterization of the charge transfer properties.

			Cu	I	N ligand	PPh3
1	S1	Hole	60.22%	31.74%	8.04%	
		Electron	4.09%	3.16%	92.75%	
		Difference*	56.13%	28.58%	-84.71%	
	T1	Hole	60.60%	32.08%	7.33%	
		Electron	3.91%	3.03%	93.06%	
		Difference	56.69%	29.04%	-85.73%	
2	S1	Hole	21.04%	65.55%	3.85%	9.56%
		Electron	4.59%	2.02%	90.39%	2.99%
		Difference	16.44%	63.53%	-86.54%	6.56%
	T1	Hole	17.90%	70.76%	3.71%	7.63%
		Electron	3.96%	1.76%	91.59%	2.69%
		Difference	13.95%	68.99%	-87.88%	4.94%

* Difference = Hole - Electron, in which positive indicates hole-rich part whereas negative electron-rich part.

Crystallographic Data

Table S4 Crystal data and structure refinement for complex 1

Identification code	1897169_CuINN
Empirical formula	$C_{18}H_{18}Cu_2I_2N_6$
Formula weight	699.26
Temperature/K	100.01(13)
Crystal system	triclinic
Space group	P-1
a/Å	7.5443(3)
b/Å	8.7471(5)
c/Å	9.5306(5)
α/°	111.300(5)
β/°	109.905(4)
γ/°	99.247(4)
Volume/Å³	521.13(5)
Z	1
ρ_{calc}g/cm³	2.228
μ/mm⁻¹	25.907
F(000)	332.0
Crystal size/mm³	0.1 × 0.08 × 0.05
Radiation	CuKα (λ = 1.54184)
2Θ range for data collection/°	11.058 to 138.488
Index ranges	-9 ≤ h ≤ 6, -10 ≤ k ≤ 10, -9 ≤ l ≤ 11
Reflections collected	5238
Independent reflections	1927 [R_{int} = 0.0621, R_{sigma} = 0.0517]
Data/restraints/parameters	1927/0/128
Goodness-of-fit on F²	1.096
Final R indexes [I>=2σ (I)]	R_1 = 0.0363, wR_2 = 0.0943
Final R indexes [all data]	R_1 = 0.0381, wR_2 = 0.0962
Largest diff. peak/hole / e Å⁻³	1.98/-0.99

Table S5 Bond lengths for complex 1

Atom	Atom	Length/Å	Atom	Atom	Length/Å
I(1)	Cu(1)	2.5934(8)	N(3)	C(8)	1.358(7)
I(1)	Cu(1)*	2.6086(8)	N(1)	C(1)	1.318(7)
Cu(1)	Cu(1)*	2.5595(14)	C(1)	C(2)	1.407(7)
Cu(1)	N(3)	2.107(4)	C(2)	C(3)	1.369(8)
Cu(1)	N(1)	2.066(4)	C(4)	C(5)	1.390(7)
N(2)	N(1)	1.359(6)	C(5)	C(6)	1.377(8)
N(2)	C(3)	1.357(6)	C(6)	C(7)	1.383(8)
N(2)	C(4)	1.419(7)	C(7)	C(8)	1.380(7)
N(3)	C(4)	1.341(6)	C(8)	C(9)	1.498(7)

*1-X, 1-Y, -Z

Table S6 Bond angles for complex 1

Atom	Atom	Atom	Angle/˚	Atom	Atom	Atom	Angle/˚
Cu(1)	I(1)	Cu(1)*	58.95(3)	C(8)	N(3)	Cu(1)	127.5(3)
I(1)	Cu(1)	I(1)*	121.05(3)	N(2)	N(1)	Cu(1)	113.1(3)
Cu(1)*	Cu(1)	I(1)*	60.23(3)	C(1)	N(1)	Cu(1)	141.8(4)
Cu(1)*	Cu(1)	I(1)	60.82(3)	C(1)	N(1)	N(2)	105.1(4)
N(3)	Cu(1)	I(1)	117.13(12)	N(1)	C(1)	C(2)	111.6(5)
N(3)	Cu(1)	I(1)*	109.07(12)	C(3)	C(2)	C(1)	104.9(5)
N(3)	Cu(1)	Cu(1)*	142.66(13)	N(2)	C(3)	C(2)	106.9(4)
N(1)	Cu(1)	I(1)*	113.58(12)	N(3)	C(4)	N(2)	114.6(4)
N(1)	Cu(1)	I(1)	110.03(12)	N(3)	C(4)	C(5)	124.1(5)
N(1)	Cu(1)	Cu(1)*	139.00(13)	C(5)	C(4)	N(2)	121.3(5)
N(1)	Cu(1)	N(3)	78.25(17)	C(6)	C(5)	C(4)	117.0(5)
N(1)	N(2)	C(4)	118.9(4)	C(5)	C(6)	C(7)	120.3(5)
C(3)	N(2)	N(1)	111.5(4)	C(8)	C(7)	C(6)	119.2(5)
C(3)	N(2)	C(4)	129.1(4)	N(3)	C(8)	C(7)	121.7(5)
C(4)	N(3)	Cu(1)	114.8(3)	N(3)	C(8)	C(9)	115.3(4)
C(4)	N(3)	C(8)	117.7(4)	C(7)	C(8)	C(9)	122.9(5)

*1-X, 1-Y, -Z

Table S7 Crystal data and structure refinement for complex 2

Identification code	1897143_CuINP
Empirical formula	$C_{27}H_{24}CuIN_3P$
Formula weight	611.90
Temperature/K	99.97(15)
Crystal system	triclinic
Space group	P-1
a/Å	8.1926(3)
b/Å	9.4737(5)
c/Å	17.6793(9)
α/°	78.611(4)
β/°	77.753(4)
γ/°	67.501(4)
Volume/Å³	1228.55(11)
Z	2
ρ_{calc}g/cm³	1.654
μ/mm⁻¹	11.886
F(000)	608.0
Crystal size/mm³	0.1 × 0.08 × 0.07
Radiation	CuKα (λ = 1.54184)
2Θ range for data collection/°	10.192 to 138.842
Index ranges	-9 ≤ h ≤ 9, -11 ≤ k ≤ 11, -20 ≤ l ≤ 21
Reflections collected	13015
Independent reflections	4542 [R_{int} = 0.0357, R_{sigma} = 0.0305]
Data/restraints/parameters	4542/0/299
Goodness-of-fit on F²	1.050
Final R indexes [I>=2σ (I)]	R_1 = 0.0278, wR_2 = 0.0717
Final R indexes [all data]	R_1 = 0.0285, wR_2 = 0.0720
Largest diff. peak/hole / e Å⁻³	1.00/-0.65

Table S8 Bond lengths for complex 2

Atom	Atom	Length/Å	Atom	Atom	Length/Å
I(1)	Cu(1)	2.6243(4)	C(8)	C(9)	1.492(4)
Cu(1)	P(1)	2.2061(7)	C(10)	C(11)	1.395(4)
Cu(1)	N(1)	2.090(3)	C(10)	C(15)	1.395(4)
Cu(1)	N(3)	2.107(2)	C(11)	C(12)	1.389(4)
P(1)	C(10)	1.833(3)	C(12)	C(13)	1.390(4)
P(1)	C(16)	1.834(3)	C(13)	C(14)	1.380(4)
P(1)	C(22)	1.832(3)	C(14)	C(15)	1.395(4)
N(1)	N(2)	1.362(3)	C(16)	C(17)	1.393(4)
N(1)	C(1)	1.319(4)	C(16)	C(21)	1.395(4)
N(2)	C(3)	1.364(4)	C(17)	C(18)	1.396(4)
N(2)	C(4)	1.409(4)	C(18)	C(19)	1.383(4)
N(3)	C(4)	1.340(4)	C(19)	C(20)	1.387(4)
N(3)	C(8)	1.350(4)	C(20)	C(21)	1.390(4)
C(1)	C(2)	1.397(5)	C(22)	C(23)	1.394(4)
C(2)	C(3)	1.356(5)	C(22)	C(27)	1.395(4)
C(4)	C(5)	1.392(4)	C(23)	C(24)	1.388(4)
C(5)	C(6)	1.380(4)	C(24)	C(25)	1.381(4)
C(6)	C(7)	1.390(5)	C(25)	C(26)	1.373(4)
C(7)	C(8)	1.388(4)	C(26)	C(27)	1.399(4)

Table S9 Bond angles for complex 2

Atom	Atom	Atom	Angle/°	Atom	Atom	Atom	Angle/°
P(1)	Cu(1)	I(1)	119.99(2)	C(8)	C(7)	C(6)	119.3(3)
N(1)	Cu(1)	I(1)	105.30(7)	N(3)	C(8)	C(7)	121.5(3)
N(1)	Cu(1)	P(1)	110.29(7)	N(3)	C(8)	C(9)	117.0(3)
N(1)	Cu(1)	N(3)	78.29(10)	C(7)	C(8)	C(9)	121.4(3)
N(3)	Cu(1)	I(1)	103.02(7)	C(11)	C(10)	P(1)	118.1(2)
N(3)	Cu(1)	P(1)	130.13(7)	C(15)	C(10)	P(1)	123.3(2)
C(10)	P(1)	Cu(1)	121.86(9)	C(15)	C(10)	C(11)	118.6(2)
C(10)	P(1)	C(16)	101.84(12)	C(12)	C(11)	C(10)	120.9(3)
C(16)	P(1)	Cu(1)	110.76(8)	C(11)	C(12)	C(13)	119.8(3)
C(22)	P(1)	Cu(1)	114.43(9)	C(14)	C(13)	C(12)	120.0(3)
C(22)	P(1)	C(10)	102.48(12)	C(13)	C(14)	C(15)	120.1(3)
C(22)	P(1)	C(16)	103.27(12)	C(14)	C(15)	C(10)	120.5(3)
N(2)	N(1)	Cu(1)	112.29(18)	C(17)	C(16)	P(1)	123.2(2)
C(1)	N(1)	Cu(1)	142.0(2)	C(17)	C(16)	C(21)	119.0(2)
C(1)	N(1)	N(2)	105.1(2)	C(21)	C(16)	P(1)	117.7(2)
N(1)	N(2)	C(3)	111.3(2)	C(16)	C(17)	C(18)	120.5(3)
N(1)	N(2)	C(4)	119.0(2)	C(19)	C(18)	C(17)	119.8(3)
C(3)	N(2)	C(4)	129.7(3)	C(18)	C(19)	C(20)	120.2(3)
C(4)	N(3)	Cu(1)	114.58(19)	C(19)	C(20)	C(21)	119.9(3)
C(4)	N(3)	C(8)	118.1(2)	C(20)	C(21)	C(16)	120.4(3)
C(8)	N(3)	Cu(1)	127.0(2)	C(23)	C(22)	P(1)	118.5(2)
N(1)	C(1)	C(2)	111.2(3)	C(23)	C(22)	C(27)	118.2(3)
C(3)	C(2)	C(1)	106.1(3)	C(27)	C(22)	P(1)	123.3(2)
C(2)	C(3)	N(2)	106.4(3)	C(24)	C(23)	C(22)	121.0(3)
N(3)	C(4)	N(2)	115.4(2)	C(25)	C(24)	C(23)	120.1(3)
N(3)	C(4)	C(5)	124.1(3)	C(26)	C(25)	C(24)	119.9(3)
C(5)	C(4)	N(2)	120.6(3)	C(25)	C(26)	C(27)	120.4(3)
C(6)	C(5)	C(4)	117.2(3)	C(22)	C(27)	C(26)	120.4(3)
C(5)	C(6)	C(7)	119.8(3)				

Table S10 Crystal data and structure refinement for complex 3

Identification code	CuIP
Empirical formula	$C_{72}H_{60}Cu_4I_4P_4 \cdot 1.2\ CH_3CN$
Formula weight	1860.17
Temperature/K	100.00(18)
Crystal system	monoclinic
Space group	C2/c
a/Å	25.9779(15)
b/Å	16.0832(5)
c/Å	18.0362(7)
α/°	90
β/°	109.224(4)
γ/°	90
Volume/Å^3	7115.5(6)
Z	4
ρ_{calc}g/cm^3	1.736
μ/mm^{-1}	16.142
F(000)	3626.0
Crystal size/mm^3	0.153 × 0.095 × 0.048
Radiation	CuKα (λ = 1.54184)
2Θ range for data collection/°	7.208 to 134.48
Index ranges	-31 ≤ h ≤ 31, -19 ≤ k ≤ 19, -21 ≤ l ≤ 19
Reflections collected	18262
Independent reflections	6303 [R_{int} = 0.0520, R_σ = 0.0660]
Data/restraints/parameters	6303/14/408
Goodness-of-fit on F^2	1.070
Final R indexes [I>=2σ (I)]	R_1 = 0.0606, wR_2 = 0.1425
Final R indexes [all data]	R_1 = 0.0735, wR_2 = 0.1498
Largest diff. peak/hole / e Å^{-3}	3.13/-2.50

Table S11 Bond lengths for complex 3

Atom	Atom	Length/Å	Atom	Atom	Length/Å
I001	Cu03*	2.6969(13)	C00F	C00P	1.364(13)
I001	Cu03	2.6982(12)	C00G	C00R	1.390(11)
I001	Cu04	2.5894(13)	C00G	C00Z	1.374(13)
I002	Cu03	2.6452(13)	C00H	C00M	1.399(13)
I002	Cu04	2.5363(12)	C00I	C00Q	1.374(12)
Cu03	Cu04	2.7798(18)	C00J	C014	1.386(13)
Cu03	P005	2.245(2)	C00K	C00Y	1.386(14)
Cu04	P006	2.229(3)	C00K	C015	1.374(14)
P005	C008	1.823(8)	C00L	C00N	1.389(13)
P005	C00A	1.823(8)	C00M	C00S	1.389(15)
P005	C00B	1.836(9)	C00N	C00W	1.389(12)
P006	C009	1.820(9)	C00O	C011	1.390(13)
P006	C00G	1.833(8)	C00P	C00X	1.368(13)
P006	C00K	1.823(8)	C00Q	C00T	1.375(12)
C007	C00B	1.383(11)	C00R	C00V	1.398(13)
C007	C00F	1.408(12)	C00S	C014	1.361(14)
C008	C00I	1.388(11)	C00T	C011	1.377(13)
C008	C00O	1.387(12)	C00U	C00V	1.380(14)
C009	C00H	1.393(12)	C00U	C013	1.391(14)
C009	C00J	1.382(13)	C00Y	C010	1.387(14)
C00A	C00C	1.401(12)	C00Z	C013	1.380(12)
C00A	C00W	1.409(11)	C010	C012	1.348(16)
C00B	C00D	1.386(13)	C012	C016	1.373(17)
C00C	C00E	1.389(12)	C015	C016	1.400(15)
C00D	C00X	1.407(12)	C1	N2	1.06(2)

*3/2-X, 3/2-Y, 1-Z

Table S12 Selected bond angles for complex 3

Atom	Atom	Atom	Angle/°	Atom	Atom	Atom	Angle/°
Cu03*	I001	Cu03	78.64(4)	C00W	C00A	P005	118.0(6)
Cu04	I001	Cu03*	105.42(4)	C007	C00B	P005	122.0(7)
Cu04	I001	Cu03	63.39(4)	C007	C00B	C00D	120.2(8)
Cu04	I002	Cu03	64.85(4)	C00D	C00B	P005	117.8(6)
I001*	Cu03	I001	101.36(4)	C00E	C00C	C00A	121.1(8)
I001	Cu03	Cu04	56.39(4)	C00B	C00D	C00X	119.7(9)
I001*	Cu03	Cu04	116.04(5)	C00L	C00E	C00C	120.3(8)
I002	Cu03	I001	111.91(5)	C00P	C00F	C007	120.2(8)
I002	Cu03	I001*	103.14(4)	C00R	C00G	P006	123.1(7)
I002	Cu03	Cu04	55.68(4)	C00Z	C00G	P006	117.3(6)
P005	Cu03	I001	113.02(6)	C00Z	C00G	C00R	119.6(8)
P005	Cu03	I001*	114.40(7)	C009	C00H	C00M	121.5(9)
P005	Cu03	I002	112.17(7)	C00Q	C00I	C008	121.9(8)
P005	Cu03	Cu04	129.56(8)	C009	C00J	C014	120.3(8)
I001	Cu04	Cu03	60.21(4)	C00Y	C00K	P006	118.3(7)
I002	Cu04	I001	119.49(5)	C015	C00K	P006	122.4(7)
I002	Cu04	Cu03	59.47(4)	C015	C00K	C00Y	119.2(9)
P006	Cu04	I001	113.27(7)	C00E	C00L	C00N	119.9(8)
P006	Cu04	I002	126.30(7)	C00S	C00M	C00H	118.7(9)
P006	Cu04	Cu03	164.73(8)	C00W	C00N	C00L	120.2(8)
C008	P005	Cu03	114.0(3)	C008	C00O	C011	120.6(9)
C008	P005	C00A	104.6(4)	C00F	C00P	C00X	121.0(8)
C008	P005	C00B	102.6(4)	C00I	C00Q	C00T	119.5(8)
C00A	P005	Cu03	114.3(3)	C00G	C00R	C00V	119.5(9)
C00A	P005	C00B	104.9(4)	C014	C00S	C00M	119.8(9)
C00B	P005	Cu03	115.0(3)	C00Q	C00T	C011	120.0(8)
C009	P006	Cu04	117.4(3)	C00V	C00U	C013	120.2(8)
C009	P006	C00G	104.1(4)	C00U	C00V	C00R	120.1(9)
C009	P006	C00K	105.9(4)	C00N	C00W	C00A	120.7(8)
C00G	P006	Cu04	114.4(3)	C00P	C00X	C00D	119.6(9)
C00K	P006	Cu04	109.3(3)	C00K	C00Y	C010	121.2(10)
C00K	P006	C00G	104.6(4)	C00G	C00Z	C013	121.5(9)
C00B	C007	C00F	119.2(9)	C012	C010	C00Y	119.1(10)
C00I	C008	P005	119.1(6)	C00T	C011	C00O	120.1(9)
C00O	C008	P005	123.2(6)	C010	C012	C016	121.0(10)

*3/2-X, 3/2-Y, 1-Z

References of ESI

1. G. M. Sheldrick, *Acta. Cryst. A*, 2008, **64**, 112-122.
2. G. Sheldrick, *Acta Cryst. C*, 2015, **71**, 3-8.
3. O. V. Dolomanov, L. J. Bourhis, R. J. Gildea, J. A. K. Howard and H. Puschmann, *J. Appl. Crystallogr.*, 2009, **42**, 339-341.
4. M. J. Frisch, G. W. Trucks, H. B. Schlegel, G. E. Scuseria, M. A. Robb, J. R. Cheeseman, G. Scalmani, V.Barone, G. A. Petersson, H. Nakatsuji, X. Li, M. Caricato, A. Marenich, J. Bloino, B. G. Janesko, R. Gomperts, B. Mennucci, H. P. Hratchian, J. V. Ortiz, A. F. Izmaylov, J. L. Sonnenberg, D. Williams-Young, F. Ding, F. Lipparini, F. Egidi, J. Goings, B. Peng, A. Petrone, T. Henderson, D. Ranasinghe, V. G. Zakrzewski, J. Gao, N. Rega, G. Zheng, W. Liang, M. Hada, M. Ehara, K. Toyota, R. Fukuda, J. Hasegawa, M. Ishida, T. Nakajima, Y. Honda, O. Kitao, H. Nakai, T. Vreven, K. Throssell, J. J. A. Montgomery, J. E. Peralta, F. Ogliaro, M. Bearpark, J. J. Heyd, E. Brothers, K. N. Kudin, V. N. Staroverov, T. Keith, R. Kobayashi, J. Normand, K. Raghavachari, A. Rendell, J. C. Burant, S. S. Iyengar, J. Tomasi, M. Cossi, J. M. Millam, M. Klene, C. Adamo, R. Cammi, J. W. Ochterski, R. L. Martin, K. Morokuma, O. Farkas, J. B. Foresman and D. J. Fox, Gaussian 09, Wallingford CT, Gaussian, Inc, 2016
5. T. Lu and F. Chen, *J. Comput. Chem.*, 2012, **33**, 580-592.
6. W. Humphrey, A. Dalke and K. Schulten, *J. Mol. Graph.*, 1996, **14**, 33-38.
7. S. Liu, X. Zeng and B. Xu, *Tetrahedron Lett.*, 2016, **57**, 3706-3710.